

THE EVOLUTION OF IRRADIATED PLANETS. APPLICATION TO TRANSITS

G. CHABRIER¹, T. BARMAN², I. BARAFFE¹, F. ALLARD¹, & P.H. HAUSCHILDT³

¹Ecole Normale Supérieure de Lyon, C.R.A.L. (UMR CNRS 5574), 69364 Lyon, France

²Wichita State University

³Hamburger Sternwarte, Hamburg, Germany

Draft version February 2, 2008

ABSTRACT

Extending the theory we derived recently for HD209458b to different cases of strongly irradiated gaseous exoplanets, we have calculated the consistent evolution of the new transiting planet, OGLE-TR-56b, for its recently revised mass determination. The theory is shown to successfully reproduce the observed radius, for the proper age of the system. We also examine the dissipation of kinetic energy at the planet's internal adiabat due to atmospheric winds, and place constraints on the efficiency of this process. We show that a fraction $\sim 0.1 - 0.5\%$ of the incident flux transformed into thermal energy deposited at the adiabatic level can accommodate the observed radii of both OGLE-TR-56b and HD209458b. The present theory yields quantitative predictions on the evolution of the emergent spectrum and fundamental properties of hot-jupiters. The predictions for radius, luminosity, temperature as a function of the planet's mass and orbital distance can be used as benchmarks for future detections of transit planets.

Subject headings: binaries: eclipsing - planetary systems - stars: individual (OGLE-TR-56, HD 209458)

1. INTRODUCTION

Since the discovery of 51 Peg b (Mayor & Queloz 1995), over a hundred gaseous planets have been discovered in orbit around G, K, and M stars. These discoveries have opened a new domain of research in astronomy, at the crossroad between stellar and planetary physics. Many ground-based and space-based missions are planned for the coming years to search for more of these objects, and the next decade will probably see the first direct detection of an extrasolar planet. These projects require a robust theoretical background to accurately understand the properties of these objects and to provide reliable guidance for observations. The vast majority of these planets have a projected mass, $m \times \sin i$, of about one Jupiter mass ($M_{jup} \simeq 10^{-3} M_{\odot}$) but are found to orbit much closer to their parent star than Jupiter, with a pile-up around $a \sim 0.04$ AU. As such, these planets experience strong irradiation from their parent star. Observations of objects that transit their parent star provide information crucial to understanding these so-called hot-jupiters. The transit light curve or photometry, supplemented by radial velocity measurements of the star, yields the absolute mass and average radius of the planet. Together with an estimate of the age of the parent star from stellar evolution models, the radius and mass provide stringent constraints on the evolution of the internal and atmospheric properties of strongly irradiated planets. The correct description of these properties has been questioned recently by the detection of the transit planet HD209458b (Brown et al. 2001). No consistent model can adequately reproduce the observationally determined mass and radius of the planet ($R_p = 1.42^{+0.10}_{-0.13} R_{jup}$) (Cody & Sasselov 2002) without stretching these determinations beyond their error bars (Guillot & Showman 2002, Baraffe et al. 2003, Burrows et al. 2003). This led to the suggestion that an important part of fundamental physics might be missing in the description of irradiated planets and has motivated several authors to propose

possible shortcomings of the theory. In the present letter, the theory developed in Baraffe et al. (2003) for non-irradiated and irradiated planets is applied to various cases of hot-jupiters, with special focus on the case of the second observed transit, OGLE-TR-56b. The theory adequately reproduces the observed radius of the planet, for the proper age of the system and the more recent mass determination (Torres et al. 2003). The comparison of the present predictions for the evolution of hot-jupiters with forthcoming transit detections will allow the unambiguous verification or rejection of the present theory.

2. EFFECT OF IRRADIATION

For a planet in close orbit around its parent star, the strong incident stellar radiation substantially modifies not only the emergent spectrum but also the evolution of the irradiated planet, as shown initially by Guillot et al. (1996). These effects are examined below.

2.1. Atmosphere

Under strong irradiation conditions, the solution of the transfer equation, which determines the atmospheric thermal structure of the planet, must include the incoming incident stellar flux in the source function. Such calculations were first conducted for hot-jupiters by Seager & Sasselov (1998), using a limited set of opacities, and have subsequently been improved by Barman, Allard & Hauschildt (2001) and Sudarsky, Burrows & Hubeny (2003). Figure 1 compares the thermal structures of irradiated and non-irradiated planets with surface gravity $\log g = 3.5$ (cgs units) and intrinsic temperatures $T_{\text{eff}} = 500$ K and $T_{\text{eff}} = 100$ K, respectively, orbiting a G2 main sequence star at 0.023 AU or 0.046 AU. The atmosphere models were produced using the same cloud-free opacity setup described by Allard et al. (2001) and Barman, Allard & Hauschildt (2001). As examined below, this T_{eff} sequence corresponds to an age sequence of $\sim 3 \times 10^7$ yr to $\sim 9 \times 10^9$ yr for OGLE-TR-56b. The irradiated thermal profile is shown to be strongly modified

with respect to the non-irradiated one. As stressed in Baraffe et al. (2003), the differences between irradiated and non-irradiated temperature profiles clearly demonstrate the necessity to do *consistent* calculations that combine the irradiated atmosphere profile and interior profile. Matching arbitrarily the inner profile to an atmospheric profile defined by the equilibrium temperature of the planet yields severely flawed results.

Note that the present calculations assume that all the incident flux is concentrated on the day-side of the planet. Such an assumption maximizes the effect of irradiation and might overestimate the flux deposit. The present nearly isothermal irradiated profiles, however, are consistent with the $2\mu\text{m}$ observed spectrum of HD209458b (Richardson, Deming & Seager 2003). Future calculations will include the latitude dependence of the incoming radiation but it is certainly interesting to verify whether the present calculations, with minimal assumptions, adequately reproduce the radius of new observed transiting planets.

2.2. Evolution

Consistent evolution calculations of irradiated planets have been conducted only recently by Baraffe et al. (2003) and Burrows et al. (2003). The calculations presented here proceed as described in Chabrier & Baraffe (1997) for the non-irradiated case. A grid of irradiated atmospheric structures is computed for various $(\log g, T_{\text{eff}})$ conditions, for a given orbital distance a , and interpolation between these structures yield the unique boundary condition with the internal structure, at large enough optical depth ($\tau \approx 100$). As shown initially by Guillot et al. (1996), irradiation pushes the radiative-convective boundary deeper into the interior and, under strong irradiation conditions, may force the boundary between the atmospheric and internal structure to lie in a radiative layer. To insure consistency between the atmosphere and internal thermal structures, we have computed the Rosseland mean of the atmospheric opacities and used this value to calculate the radiative gradient for the interior structure. The evolution of the planet obeys the usual first and second principles of thermodynamics. The energy balance, however, must include the incoming stellar radiative flux $\mathcal{F}_{\text{inc}} = 1/2(R_*/a)^2 \mathcal{F}_*$, where \mathcal{F}_* and R_* denote the parent star flux and radius, respectively. The total emergent flux of the planet \mathcal{F}_{out} now reads :

$$\begin{aligned} \mathcal{F}_{\text{out}} &= \mathcal{F}_{\text{inc}} + \sigma T_{\text{eff}}^4 \\ &= A \mathcal{F}_{\text{inc}} + (1 - A) \mathcal{F}_{\text{inc}} + \sigma T_{\text{eff}}^4 \end{aligned} \quad (1)$$

where T_{eff} denotes the intrinsic effective temperature of the planet, A its Bond albedo, and the first term on the r.h.s. of eqn.(1) describes the reflected part of the spectrum. Note that the albedo A is not a free parameter in our calculations but is calculated consistently with the radiative transfer equation. For both transit cases, the models predict $A < 0.1$. The total luminosity thus reads:

$$\begin{aligned} L_{\text{tot}} &= L_{\text{reflected}} + 4\pi R_p^2 \sigma (T_{\text{eq}}^4 + T_{\text{eff}}^4) \\ &= L_{\text{reflected}} + 4\pi R_p^2 \sigma T_{\text{eq}}^4 - \int T \frac{dS}{dt} dm \end{aligned} \quad (2)$$

where S denotes the specific entropy of the planet. Whereas the total flux \mathcal{F}_{out} or luminosity L_{tot} is the quantity accessible to observation, only the last term on the right hand side of eqn.(2) concerns the evolution of the planet intrinsic luminosity L_{int} . The first term, which defines the Bond albedo, illustrates the fraction of the stellar luminosity reflected by the planet atmosphere. The second term defines its equilibrium temperature, i.e. the temperature the planet would reach in the absence of any internal source of energy ($T_{\text{eff}} \rightarrow 0$). Figure 2 compares the emergent flux calculated for OGLE-TR-56b and HD209458b at their present ages. In both cases, the infrared part of the spectrum ($\gtrsim 1\mu\text{m}$) is dominated by the re-radiation of the absorbed incident stellar flux. Indeed, under the conditions of interest, this contribution largely dominates the intrinsic contribution of the planet ($T_{\text{eq}} \simeq 2400\text{ K} \gg T_{\text{eff}} \simeq 100\text{ K}$ for OGLE-TR-56b, and $T_{\text{eq}} \simeq 1700\text{ K} \gg T_{\text{eff}} \simeq 100\text{ K}$ for HD209458b). For HD209458b, the short wavelength part of the spectrum ($\lesssim 0.5\mu\text{m}$) is mostly due to reflection of stellar light by H_2 Rayleigh scattering. However, in OGLE-TR-56b the high equilibrium temperature, $T_{\text{eq}} = 2400\text{ K}$, leads to a lower concentration of H_2 . Consequently, reflection is less significant and the majority of the spectrum of OGLE-TR-56b is thermal radiation.

Figure 3 displays the evolution of the radius for different strongly irradiated planet conditions, with masses $0.69 M_{\text{Jup}}$ and $1.5 M_{\text{Jup}}$, orbiting a G2 star ($T_{\text{eff}} = 5900\text{ K}$) at different orbital distances, namely $a = 0.046\text{ AU}$ and $a = 0.023\text{ AU}$. At a given orbital distance, the less massive the planet the larger the effect of irradiation. This was expected from Figure 1, showing the larger modification of the inner atmosphere profile with larger stellar/planet flux ratio. In all cases, however, irradiation substantially slows down the contraction of the planet, in particular at the early stages of evolution, when degeneracy effects in the interior are smaller. The case $m = 1.5 M_{\text{Jup}}$ and $a = 0.023\text{ AU}$ (thick solid line) corresponds to OGLE-TR-56b, for its recently revised mass, $m \simeq 1.45 \pm 0.23 M_{\text{Jup}}$, and radius $1.23 \pm 0.15 R_{\text{Jup}}$ (Torres et al. 2003). The age of the system was derived from the evolution of the parent star for its observed extinction-corrected magnitude and effective temperature (Sasselov 2003). We derive $m \simeq 1.05 M_{\odot}$, $t \sim 4\text{ Gyr}$ to reproduce the observations, in excellent agreement with Sasselov (2003). The striking result is the very good agreement, within the error bar, between the present calculations and the observations. A prediction of the theory is that irradiation from a G2 star yields less than about 15% increase of the planet radius after $\sim 1\text{ Gyr}$, compared with the non-irradiated case, with all radii merging within the $\sim 1.1\text{--}1.15 R_{\text{Jup}}$ range at this stage. A key test for the theory, however, would be the observation of young ($\lesssim 10^9\text{ yr}$) transits, where radii of irradiated planets are predicted to vary rapidly with time and to depend substantially on the orbital distance.

The case of HD209458b thus becomes a puzzle. As discussed at length in Baraffe et al. (2003), no consistent evolution calculation can reproduce the observed radius. Note that our calculations take into account the extension of the atmosphere, which we find to be of the order of $\sim 0.05 R_{\text{Jup}}$ (at optical wavelengths) for the age of this object. Given the remaining uncertainties

in the opacities of these planets, including for example non-equilibrium processes or day-night temperature gradients, we cannot exclude larger extensions. It is very unlikely, however, that different opacities modify the internal adiabat strongly enough to increase the planet radius by 30% and thus solve the aforementioned discrepancy between theory and observation for HD209458b. Such a modification requires a drastic change of the energy deposited at the top of the internal adiabat, which essentially determines the radius (Baraffe et al. 2003, Guillot & Showman 2002). Molecular absorption, however, will prevent incident photons from penetrating that deep ($T \sim 2000$ K near the top of the internal adiabat, see Figure 1). As discussed in §4.3 of Baraffe et al. (2003), dynamical processes such as tidal dissipation or synchronization are unlikely to provide the extra source of energy, for these timescales are at most of the order of 10^8 yr. An interesting alternative scenario involves the inner redistribution of large scale atmospheric kinetic energy (winds) generated by the incident irradiation (Guillot & Showman 2002, Showman & Guillot 2002). Besides arbitrarily modifying the atmosphere-interior boundary condition, however, these calculations face a similar issue as mentioned above, namely about 1% of this kinetic energy must *constantly* be dissipated at the internal adiabat level, i.e. $P \sim 500$ bar for HD209458b (see Figure 5 of Baraffe et al. 2003) and $\sim 4 \times 10^3$ bar for OGLE-TR-56b (see Figure 1). This corresponds to 18 and 23 pressure scale heights for these two planets, respectively. Whether such a fraction of the surface flux of kinetic energy can be transported downward over so many scale heights and converted into thermal energy remains to be uniquely determined.

In order to test this scenario in the case of OGLE-TR-56b, we have made evolution calculations where a fraction of the incident stellar flux is deposited deep enough in the planet to modify its internal adiabat (see Baraffe et al. 2003). Figure 4 displays the evolution for the two transiting planets when a fraction $X_\star = \mathcal{F}_{dep}/\mathcal{F}_{inc}$ of the incident flux over the day-side surface is deposited in the interior, with $X_\star \simeq 0.1\%$ to 1 or 2%. These values correspond to about 40 to 400 times the planet's intrinsic energy flux for OGLE-TR-56b and up to about 2000 times for HD209458b. As shown in the figure, *if* indeed OGLE-TR-56b is unambiguously confirmed as a transiting planet, values of X_\star larger than $\sim 0.5\%$ seem to be excluded, for they yield an interior entropy and radius that are too large. For HD209458b, on the contrary, $X_\star = 0.5\%$ is about the minimum fraction needed to be consistent with the observational error bar. As shown earlier, however, the internal adiabat for the HD209458b irradiation conditions lies at fewer pressure scale heights from the surface than for OGLE-TR-56b so that we expect intuitively a larger fraction of energy to be transported downward. Although these conclusions must be considered with caution, they suggest that the dissipative process invoked by Showman & Guillot may indeed take place in hot-jupiters. A tiny ($\lesssim 0.5\%$) fraction of the surface kinetic flux transported downward and converted into thermal energy at the planet's radiative-convective boundary is enough to modify significantly its internal adiabat and thus its contraction rate. The

result would be a total $\sim 20\text{-}30\%$ increase of the radius, instead of the aforementioned $\sim 15\%$ increase due to bare insulation. Another appealing alternative solution to the HD209458b dilemma is the suggestion by Bodenheimer, Laughlin & Lin (2003) of a second orbiting planet, forcing the finite eccentricity ($e \sim 0.03$) of HD209458b. The constant tidal heating due to the orbit circularization could provide the required mysterious extra source of energy.

This key issue will be nailed down in the near future with further observations of transits, as planned with the various ground-based (STARE, VULCAN) and spaced-based (COROT, MONS, MOST) missions.

3. CONCLUSION

In this letter, we have extended the theory we derived recently for the evolution of HD209458b to various conditions of so-called hot-jupiters, i.e. gaseous planets in close enough orbit around their parent star for the incoming stellar irradiation to affect substantially their structure and evolution. As argued previously, a consistent treatment between the atmospheric profile and the interior profile is mandatory to yield reliable results, both in the irradiated and non-irradiated case. The theory, in its most simple foundation (1D irradiation, with incoming flux deposited uniformly over the day side and no dynamical redistribution of the incident flux due to day-night temperature differences) is found to adequately reproduce the radius of OGLE-TR-56b. These conclusions, of course, rely on OGLE-TR-56b being a genuine exoplanet. Recent high resolution spectroscopic observations seem to support this conclusion (Konacki et al. 2003). If OGLE-TR-56b is confirmed to be, unambiguously, a planet, then the present results add intriguing support to the suggestion that the large radius of HD209458b might be due to ongoing tidal interaction with an undetected companion. However, we show that a very small fraction of the stellar incident flux, transformed into large scale kinetic energy partly dissipated at the internal adiabatic level, is sufficient to modify substantially a planet's internal entropy rate and thus evolution. This fraction is unlikely to be larger than a few 0.1%, but certainly depends on the irradiation conditions. A fraction ~ 0.1 to 0.5 % would superbly reproduce the observations of the two presently detected transits, OGLE-TR-56b and HD209458b. The present theory allows us to derive the fundamental properties of hot-jupiters (mass, temperature, radius) and their observable spectroscopic or photometric signatures as a function of age and orbital distance. Additional transit detections will also allow better constraints on possible irradiation induced dissipative processes, as explored in this letter. Comparisons between the present evolution theory and transit or direct detections of exoplanets will greatly improve our understanding of these objects and provide strong motivation for exploring this exciting new field of astronomy.

Part of this work was conducted at the Anglo-Australian Observatory, under the auspice of the franco-australian PICS program. This research was supported in part by the LTSA grant NAG 5-3435 to Wichita State University.

REFERENCES

- Allard, F., Hauschildt, P., Alexander, D., Tamanai, A., & Schweitzer, A., 2001, *ApJ*, 556, 357
- Baraffe, I., Chabrier, G., Barman, T., Allard, F., & Hauschildt, P., 2003, *A&A*, 402, 701
- Barman, T., Allard, F., Hauschildt, P., 2001, *ApJ*, 556, 885
- Bodenheimer, P., Laughlin, G., & Lin, D., 2003, *ApJ*, 592, 555
- Brown, T., Charbonneau, D., Gilliland, R., Noyes, R., & Burrows, A., 2001, *ApJ*, 552, 699
- Burrows, A., Sudarsky, D., Hubbard, W.B., 2003, *ApJ*, 594, 545
- Chabrier, G., & Baraffe, I., 1997, *A&A*, 327, 1039
- Cody, A.M., & Sasselov, D.D., 2002, *ApJ*, 569, 451
- Guillot, T., Burrows, A., Hubbard, W.B., Lunine, J.I., & Saumon, D., 1996, *ApJ*, 459, L35
- Guillot, T., & Showman, A., 2002, *A&A*, 385, 156
- Mayor, M., & Queloz, D., 1995, *Nature*, 378, 355
- Konacki, M., Torres, G., Sasselov, D., & Jha, S., 2003, *ApJ*, 597, 1076
- Richardson, L.J., Deming, D., & Seager, S., "Extrasolar Planets, Today and Tomorrow", *ASP Conf. Ser.*, in press
- Sasselov, D., 2003, *ApJ*, 596, 1327
- Showman, A., & Guillot, T., 2002, *A&A*, 385, 166
- Seager, S., & Sasselov, D., 1998, *ApJ*, 520, L157
- Sudarsky, D., Burrows, A., & Hubeny, I., 2003, *ApJ*, 1121, 588
- Torres, G., Konacki, M., Sasselov, D., & Jha, S., 2003, *ApJ*, submitted

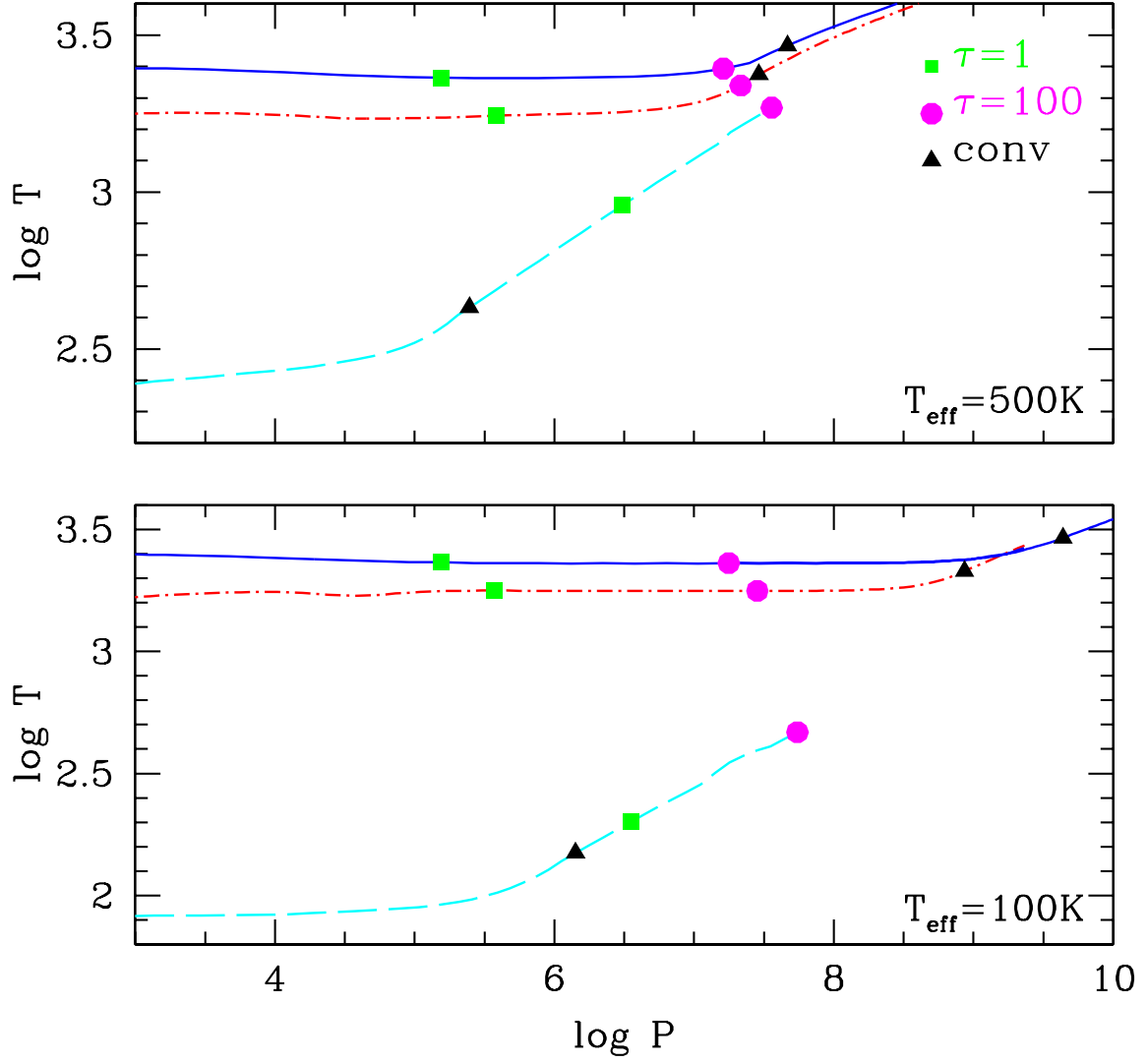


FIG. 1.— Atmospheric profiles (P in cgs units) down to the internal adiabat for non-irradiated (long-dash line) and irradiated planets with $T_{\text{eff}} = 500 \text{ K}$ and $T_{\text{eff}} = 100 \text{ K}$, $\log g = 3.5$ orbiting a G2 star at different orbital distances: $a = 0.046 \text{ AU}$ (dash-dot line) and $a = 0.023 \text{ AU}$ (solid line). Symbols indicate various optical depths (defined at $\lambda = 1.2 \mu\text{m}$) and the top of the convective zone.

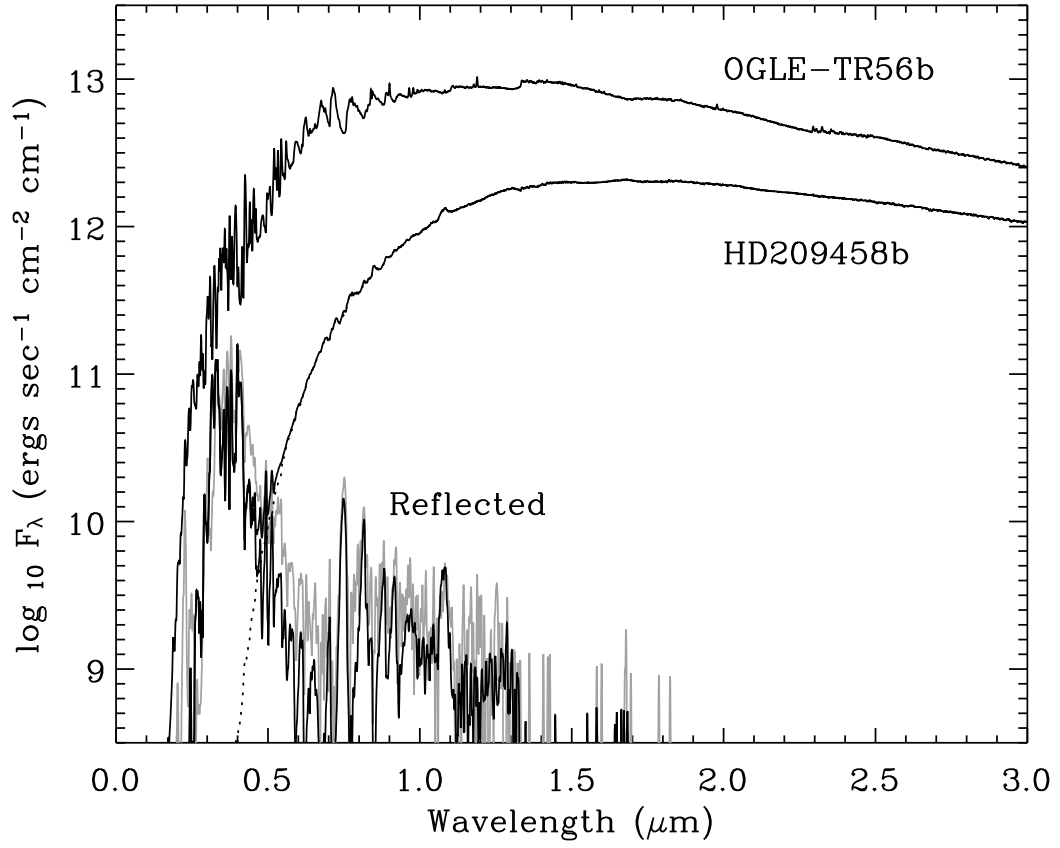


FIG. 2.— The emergent fluxes for $T_{\text{eff}} = 100$ K irradiated models corresponding to OGLE-TR-56b ($\log g = 3.5$) and HD209458b ($\log g = 3.0$). The lower two curves that peak between 0.3 and 0.4 μ m are the reflected fluxes for OGLE-TR-56b (grey) and HD209458b (black). The dotted line is the continuation of the thermal flux for HD209458b. All spectra have been reduced to a resolution of 20Å.

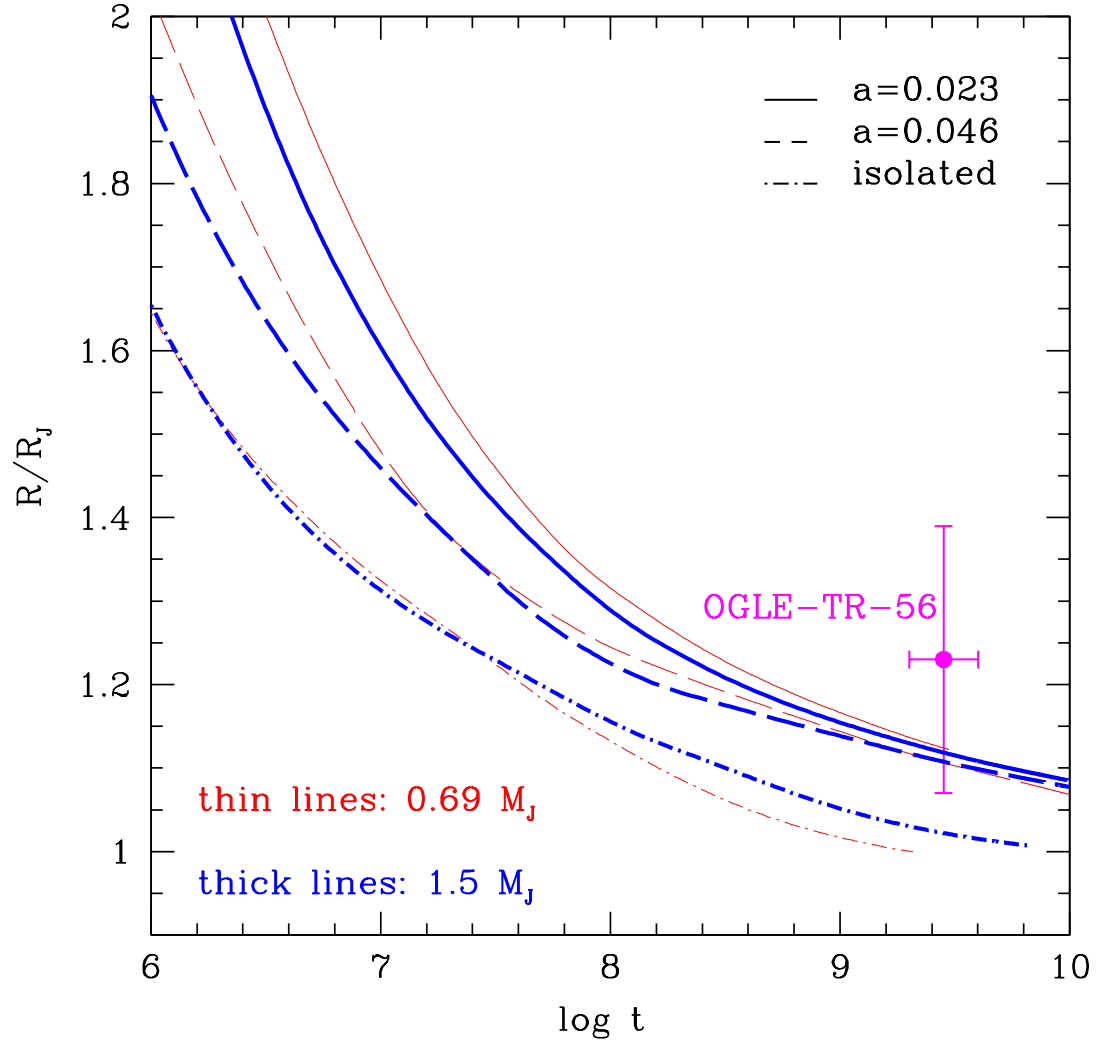


FIG. 3.— Evolution of the radius, in units of Jupiter radii, of irradiated planets with different mass: $m=0.69 M_{Jup}$ (thin lines) and $m=1.5 M_{Jup}$ (thick lines), orbiting a G2 star at different orbital distances: $a = 0.023$ AU (solid lines) and $a = 0.046$ AU (dashed lines). The case $1.5 M_{Jup}$, $a=0.023$ corresponds to OGLE-TR-56b. Dash-dotted curves display the evolution in the non-irradiated case, corresponding to planets far away from their parent star ($a \gg 1$ AU).

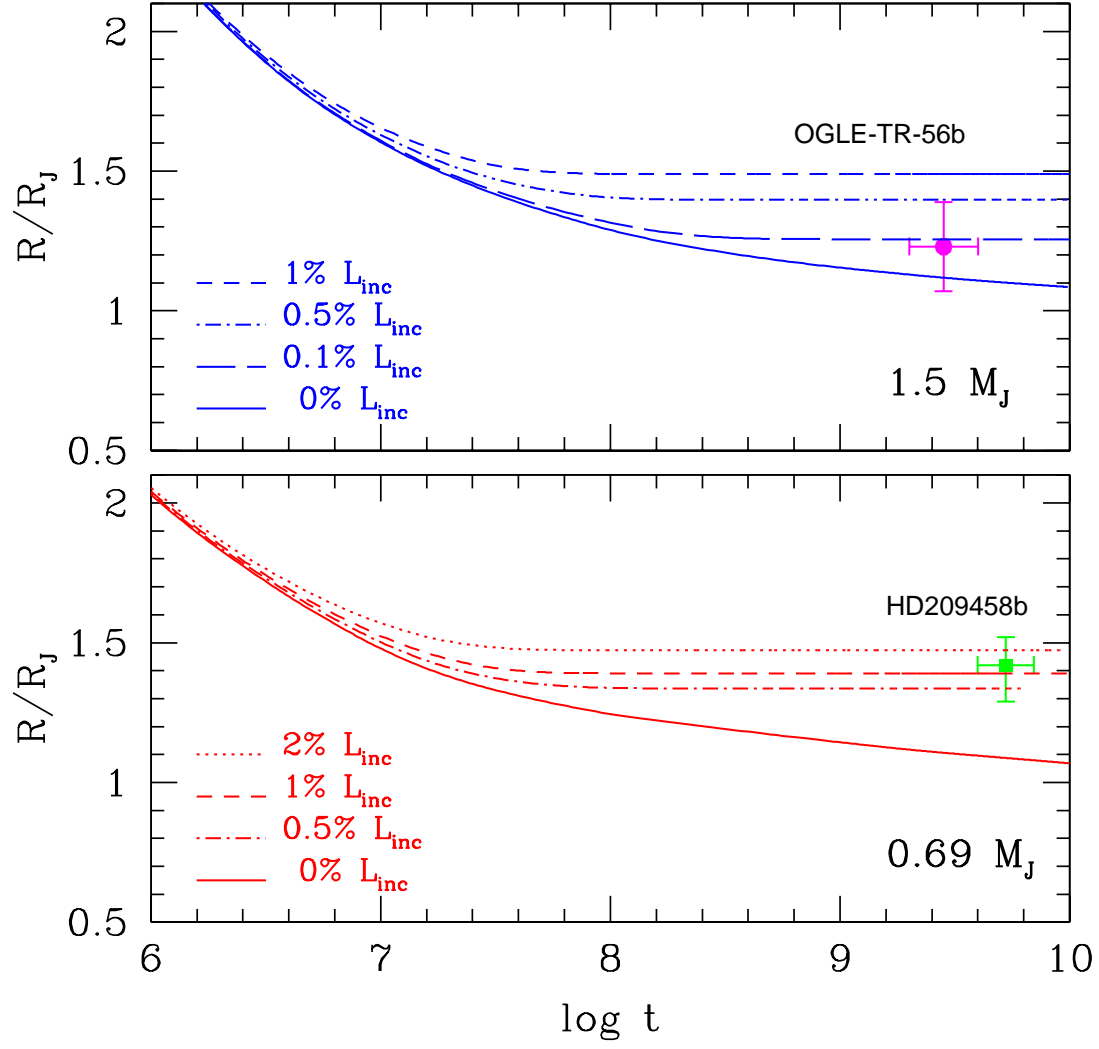


FIG. 4.— Same as Figure 3 when various fractions of the incident luminosity L_{inc} are included as an extra source of energy in the planet interior. The cases are representative of OGLE-TR-56b (upper panel) and HD209458b ($0.69 M_J$, $a=0.046$, lower panel). The 0% case (solid lines) correspond to the standard irradiated case. Note that L_{inc} is ~ 4 times larger in the case of OGLE-TR-56b than for HD209458b.